

RSC Advances



This is an *Accepted Manuscript*, which has been through the Royal Society of Chemistry peer review process and has been accepted for publication.

Accepted Manuscripts are published online shortly after acceptance, before technical editing, formatting and proof reading. Using this free service, authors can make their results available to the community, in citable form, before we publish the edited article. This *Accepted Manuscript* will be replaced by the edited, formatted and paginated article as soon as this is available.

You can find more information about *Accepted Manuscripts* in the [Information for Authors](#).

Please note that technical editing may introduce minor changes to the text and/or graphics, which may alter content. The journal's standard [Terms & Conditions](#) and the [Ethical guidelines](#) still apply. In no event shall the Royal Society of Chemistry be held responsible for any errors or omissions in this *Accepted Manuscript* or any consequences arising from the use of any information it contains.

Self-assembled triphenylamine-based fluorescent chemosensor for selectively detection of Fe³⁺ and Cu²⁺ ions in aqueous solution

Li Wengfeng, Ma Hengchang^{*a}, Lu con, Ma Yuan, Qi Chunxuan, Zhang Zhonwei, Yang Zengming, Cao Haiying, Lei ziqiang^{*b}

A novel triphenylamine-based fluorescent sensor tris((4-amino)phenylduryl)amine (*m*-TAPA) for Fe³⁺ / Cu²⁺ ion has been developed. *m*-TAPA shows high selectivity and sensitivity toward Fe³⁺ / Cu²⁺ over alkali and transition metal ions in aqueous solution. The possible mechanism of fluorescence quenching was that Fe³⁺ / Cu²⁺ can be captured by the NH₂ groups of *m*-TAPA to form non-fluorescent complexes, resulting in a strong quenching. The detection limits of Fe³⁺ and Cu²⁺ were calculated to be 230 nM and 620 nM, respectively. Furthermore, fluorescent test strips have been prepared for convenient detection of Fe³⁺ and Cu²⁺ ions in environmental water samples, even in drinking water.

1. Introduction

The detection of metal ions is very important for analytical, environmental and biomedical applications due to their deleterious effects on human health and ecosystems.^[1-3] Up to now, numerous methods have been developed for the detection of metal ions, such as atomic absorption spectroscopy^[4], colorimetric^[5], mass spectrometry^[6], electrochemical^[7,8] and fluorescence spectroscopic analysis^[9]. Among these methods, fluorescence detection attracted the most attention due to its ease of operation, high sensitivity and efficiency. Therefore, the design of fluorescent sensors for metal ions have attracted increasing attentions.

The removal of trace amounts of transition metal ions in all types of water sources is an important factor in monitoring environmental pollution. Furthermore, identifying metal-contaminated sewage and fertilizer is useful in limiting human exposure to such harmful chemicals. Copper is a major trace metal in the environment due to its extensive use in electrical and electronic industry, and poses a serious environmental threat at high levels due to its toxicity.^[10-13] The high level of copper causes neurodegenerative diseases such as Alzheimer's, Parkinson's and is also suspected to cause amyloid precipitation and toxicity.^[14-17] According to the U.S. Environmental Protection Agency (EPA), the maximum acceptable level of Cu²⁺ in drinking water is ~20 μM.^[18] Iron (Fe) also is an important limiting trace metal nutrient in natural water, as it limits the growth of phytoplankton and biomass production in rivers and lakes. High quantities (200 μg/L to 1000 μg/L) of Fe³⁺ ion in drinking water, can devastate the central nervous system, kidney, liver, skin, lungs, and bones.^[19-21] Thus, there is considerable interest in developing fluorescent sensors for the detection of Cu²⁺ and Fe³⁺ ions have been catching considerable attention in the human health and environmental science.^[22,23]

A number of fluorescent Cu²⁺^[24-28] and Fe³⁺^[29-34] sensors have been reported, and some of them have been successfully applied both in biological and in environmental samples. In addition,

^{*a} Key Laboratory of Eco-Environment-Related Polymer Materials of Ministry of Education, College of Chemistry and Chemical Engineering, Northwest Normal University, Lanzhou 730070, Gansu, China. E-mail: mahczju@hotmail.com

^{*b} Key Laboratory of Eco-Environment-Related Polymer Materials of Ministry of Education, College of Chemistry and Chemical Engineering, Northwest Normal University, Lanzhou 730070, Gansu, China. E-mail: leizq@nwnu.edu.cn

single probes for multiple targets have been actively developed because of the advantages such as potential cost and analytical time reduction. For example, they include Cr/Al^[35], Cu/Hg^[36], Cu/Zn^[37], Zn/Cd^[38], Ag/Mn^[39], Al/Fe^{3+[40]}, Cr/Fe^{3+[41]} and Zn/Al^[42]. However, single Self-assembled chemosensors for Cu²⁺ / Fe³⁺ were reported very rare^[43,44].

Herein, *m*-TAPA was synthesized by the Suzuki-Miyaura coupling reaction^[45] for multiple analytes, which can detect Cu²⁺ / Fe³⁺ ions selectively in presence of other metal ions. This is first time we reported the fluorescent sensor *m*-TAPA detect Cu²⁺ / Fe³⁺ ions in aqueous solution at nanomolar level.

2. Experimental

Materials

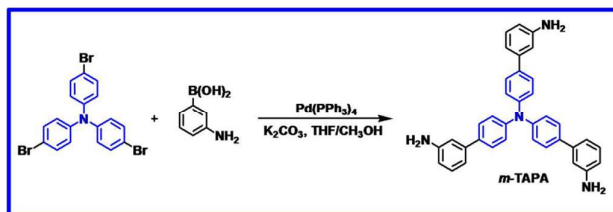
Tris(4-bromophenyl)amine (TBPA, 98%) was purchased from Energy Chemical Company. 3-Aminophenylboronic acid monohydrate (98%), was purchased from Sukailuchem Company. Terakis(triphenylphosphine)palladium(0) [Pd(PPh₃)₄] (99.8%) were purchased from Aladdin Company. Nitrogen with a purity of 99.99% was provided from commercial source. Other reagents, such as Potassium carbonate, acetonitrile, methanol, tetrahydrofuran (THF), ethyl acetate, Dichloromethane (DCM) were A.R. grade. Al(NO₃)₃·9H₂O, Mg(NO₃)₂·6H₂O, Zn(CH₃COO)₂, FeCl₂·4H₂O, SnCl₂·2H₂O, Fe₂(SO₄)₃·4H₂O, SbCl₃, K₂(SO₄), Zr(NO₃)₄·5H₂O, Ag(CH₃COO), InCl₃·4H₂O, NiCl₂·6H₂O, La(NO₃)₃·nH₂O, LiBr·H₂O, CuCl₂·2H₂O and CdNO₃·4H₂O were purchased from Aladin Ltd.(Shanghai, China). All the other chemicals were analytical grade and used as received. The aqueous solutions were prepared with twice-distilled water in the whole experiments.

Characterization

¹H NMR, ¹³C NMR were recorded on a Bruker AM 400, 100 MHz spectrometer at 25 °C. Mass spectra were recorded on a HP5989B mass spectrometer. Mass spectra were recorded on a HP5989B mass spectrometer. Fourier transform infrared (FT-IR) spectra were recorded on a DIGIL FTS3000 spectrophotometer using KBr tablets. UV spectra were measured on a TU-1901 spectrophotometer. Fluorescence spectra in solution were measured using a PE LS-55 Luminescence/Fluorescence Spectrophotometer (1%, E_x Slide: 4 nm, E_m Slide: 6 nm, Excitation: 360 nm). The morphology of TMCA was observed by scanning electron microscopy (SEM, ZEISS ULTRA PLUS).

Synthetic

The synthesis of *m*-TAPA is shown in **Scheme 1**. Synthesis of *m*-TAPA: 76% yield as slight yellow solid; R_f = 0.35 (petroleum ether : Ethyl acetate = 2:1); Mp 250-252 °C; ¹H NMR (400 MHz, CDCl₃): δ = 7.47 [*d*, 2H, ArH], δ = 7.21-7.19 [*d*, 3H, *J* = 6 Hz, ArH], 7.00-6.98 [*d*, 1H, *J* = 6 Hz, ArH], 6.90 [*s*, 1H, ArH], 6.67-6.65 [*s*, 1H, *J*=6Hz ArH], 3.73 [*s*, 2H, NH]; ¹³C NMR (DMSO-*d*₆): 149.07, 140.28, 135.60, 131.36, 129.36, 127.50, 123.99, 114.02, 112.88, 111.75; IR: 696, 781, 1284, 1319, 1485, 1599, 3013, 3358, 3442 cm⁻¹; TOF MS ES⁺: 518.25 (M+1)⁺; Elemental analysis: Calcd. for C₃₆H₃₀N₄: C 83.37; H 5.83; N 10.80; Found: C 83.20 %; H 5.85 %; 10.69% .



Scheme 1. Synthetic route to *m*-TAPA.

Fluorescence measurements Fe^{3+} and Cu^{2+}

A fixed concentration of *m*-TAPA was transferred to a fluorescent cuvette. The fluorescent intensity of the solution was recorded from 330 to 560 nm with excitation wavelength fixed at 360 nm. After appropriate amount of $\text{Fe}^{3+}/\text{Cu}^{2+}$ ions was titrated, the fluorescent intensity of the solution was again recorded. Similar procedure was performed for other metal ions. For the sake of comparison, the volume of *m*-TAPA solution was fixed to be 2 mL before the addition of $\text{Fe}^{3+}/\text{Cu}^{2+}$. All measurements were made at room temperature.

Principles of fluorescence quenching

Fluorescence quenching usually originated from collisional or dynamic quenching. Dynamic quenching can be described by the following Stern-Volmer equation.^[46] $F_0/F = \tau_0/\tau = 1 + K_q \tau_0 [Q]$ (1) where F_0 and F are the fluorescence intensities before and after the addition of the quencher, respectively. K_q is the rate constant of dynamic (collisional) quenching; τ_0 is the lifetime of the fluorophore in the absence of the quenchers; τ the lifetime in the presence of quenchers, and $[Q]$ is the quencher concentration in solution.

Another type of quenching (static quenching) occurs as a result of the formation of a non-fluorescent complex between the fluorophore and quencher. For this type of quenching, the decrease of fluorescence intensity has the same form as the Stern-Volmer equation above. However, in Eq. $F_0/F = 1 + K_{SV} [Q]$ (2), the K_{SV} is now the association constant K_S . Since the lifetime of the fluorophore is unperturbed by the static quenching, $\tau_0/\tau = 1$, lifetime measurements are a definitive method to distinguish between static and dynamic quenching.^[46]

Selectivity and interference measurements

The selectivity of *m*-TAPA was examined by the interfered metal ions such as Mg^{2+} , Zn^{2+} , K^+ , Ag^+ , Ni^{3+} , La^{3+} , Li^+ , Cd^+ , Sn^{2+} , In^{3+} , Fe^{2+} , Zr^{4+} and Al^{3+} under the identical conditions. The concentrations of Fe^{3+} (5 equiv.), Cu^{2+} (10 equiv.) and other metal ions were the same concentration. Meanwhile, for studying the interference, the *m*-TAPA was mixed with $\text{Fe}^{3+}/\text{Cu}^{2+}$ in the absence or presence of the interferent.

3. Result and discussion

The selective detection of environmentally active metal ions is investigated by visual, optical, fluorescence spectroscopy method. The *m*-TAPA was prepared in 5×10^{-5} M concentration in CH_3CN and all metal ions were prepared in 5×10^{-5} M concentration in H_2O . *m*-TAPA was treated with various metal ions like Mg^{2+} , Zn^{2+} , K^+ , Ag^+ , Ni^{3+} , La^{3+} , Li^+ , Cd^+ , Sn^{2+} , In^{3+} , Fe^{2+} , Zr^{4+} , Al^{3+} , Cu^{2+} and Fe^{3+} to study the sensitivity and selectivity towards particular metal ions over other metal ions. For the addition of 200 μL of all metal ions into *m*-TAPA, the presence of Cu^{2+} ion shows colorimetric turn-off response from colorless to brown for *m*-TAPA (**Fig. 1a**), which could be easily distinguished by 'naked-eye'. The other metal ions like Mg^{2+} , Zn^{2+} , K^+ , Ag^+ , Ni^{3+} , La^{3+} , Li^+ ,

Cd^+ , Sn^{2+} , In^{3+} , Fe^{2+} , Zr^{4+} , Al^{3+} , Sb^{3+} and Fe^{3+} with m -TAPA did not show any color change. Therefore Cu^{2+} ion could be easily identified among all other metal ions under visible light. In order to determine the amount of Fe^{3+} ion required, the color change photographs for Fe^{3+} and the other metal ions under illumination with a 365 nm UV lamp as shown in **Fig. 1b**, it is clear that fluorescence intensity quenching of m -TAPA by Cu^{2+} and Fe^{3+} ion and Fe^{3+} with m -TAPA did not show any color change indicating its effectiveness to detect Fe^{3+} over other metal ions.



Fig. 1 Color (a) and fluorescence (b) changes of m -TAPA (5×10^{-5} M solution in CH_3CN , 2 mL) after the addition of 200 μL of respective metal ions (5×10^{-5} M solution in H_2O).

Selectivity is a very important factor to estimate the performance of a new fluorescent sensor. The UV-vis spectra of m -TAPA shows strong absorption band at 340 nm. **Fig. 2** shows the absorption spectrum of m -TAPA with metal ions in aqueous medium. With the addition of $\text{Fe}^{3+}/\text{Cu}^{2+}$ into sensor m -TAPA, the intensities of the bands 340 nm (m -TAPA) have been reduced. However, the other metal ions like Mg^{2+} , Zn^{2+} , K^+ , Ag^+ , Ni^{3+} , La^{3+} , Li^+ , Cd^+ , Sn^{2+} , In^{3+} , Fe^{2+} , Zr^{4+} , Al^{3+} and Sb^{3+} did not show any optical changes with m -TAPA. From this, it is clear that m -TAPA can detect Fe^{3+} and Cu^{2+} selectively in presence of other metal ions.

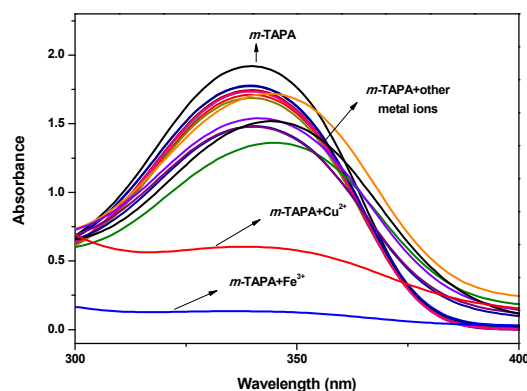


Fig. 2 UV-vis spectra of sensor m -TAPA (5×10^{-5} M, in CH_3CN) upon titration with aqueous solution of metal ions (S= m -TAPA, S+ Mg^{2+} , S+ Zn^{2+} , S+ K^+ , S+ Ag^+ , S+ Ni^{3+} , S+ La^{3+} , S+ Li^+ , S+ Cd^+ , S+ Sn^{2+} , S+ In^{3+} , S+ Fe^{2+} , S+ Zr^{4+} , S+ Al^{3+} , S+ Sb^{3+} , S+ Cu^{2+} and S+ Fe^{3+}).

Highly selective detection of Fe^{3+} and Cu^{2+} ions over other potentially competing species is a necessity. The fluorescence sensing selectivity of m -TAPA for metal ions was examined. Under the same condition as used above for Fe^{3+} and Cu^{2+} , we tested the fluorescence responses of m -TAPA toward 16 kinds of metal ions such as Mg^{2+} , Zn^{2+} , K^+ , Ag^+ , Ni^{3+} , La^{3+} , Li^+ , Cd^+ , Sn^{2+} , In^{3+} , Fe^{2+} , Zr^{4+} , Al^{3+} , Sb^{3+} , Cu^{2+} and Fe^{3+} . Metal ions were added to CH_3CN solutions of the m -TAPA (5×10^{-5} M), and the emission of the m -TAPA was measured immediately after the addition of metal ions. As shown in **Fig. 3**, among the metal ions studied, a clear fluorescence

quenching is observed upon the addition of 200 μL of Cu^{2+} and Fe^{3+} ions into *m*-TAPA. The quenching efficiency of *m*-TAPA toward Fe^{3+} and Cu^{2+} were found to be 99% and 96% respectively (Fig. 4). So, we further investigated the *m*-TAPA sensing behavior to two kinds of metal ions in aqueous solution.

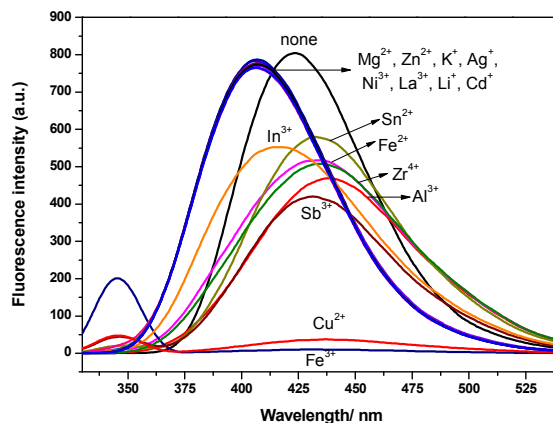


Fig. 3 Fluorescence spectra of *m*-TAPA (5×10^{-5} M, in CH_3CN) upon titration with aqueous solution of cations.

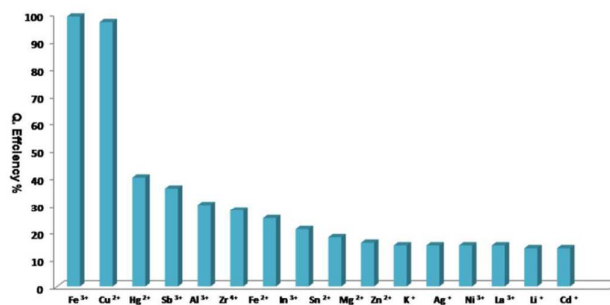


Fig. 4 The relative fluorescence quenching degree of *m*-TAPA at 425 nm with various metal ions (200 μL).

The fluorescence titration for *m*-TAPA with Fe^{3+} and Cu^{2+} ions reveals that fluorescence emission intensity rapidly died down upon addition of increasing amounts of Fe^{3+} / Cu^{2+} solution at 425 nm (Fig. 5a and 5b). Furthermore, the emissive property study disclosed that the fluorescence quantum yields of *m*-TAPA, *m*-TAPA- Fe^{3+} and *m*-TAPA- Cu^{2+} complexes are 41% , 0.6% and 1.5% , respectively [47]. The gradual addition of Fe^{3+} / Cu^{2+} into *m*-TAPA, the fluorescence band at 425 nm shifted (red Shift) to ~ 462 nm and ~ 431 nm, respectively. The result revealed the coordination ability of Fe^{3+} ion with the amine better than Cu^{2+} ion. Interestingly, a new emission band is generated at ~ 362 nm which increases with Fe^{3+} / Cu^{2+} concentration.[48] This result also indicate that Fe^{3+} / Cu^{2+} complex of *m*-TAPA is formed. A plot of fluorescence intensity depending on the concentration of Fe^{3+} / Cu^{2+} in the range from 0 to 10 equiv as shown in Fig. 5c and 5d.

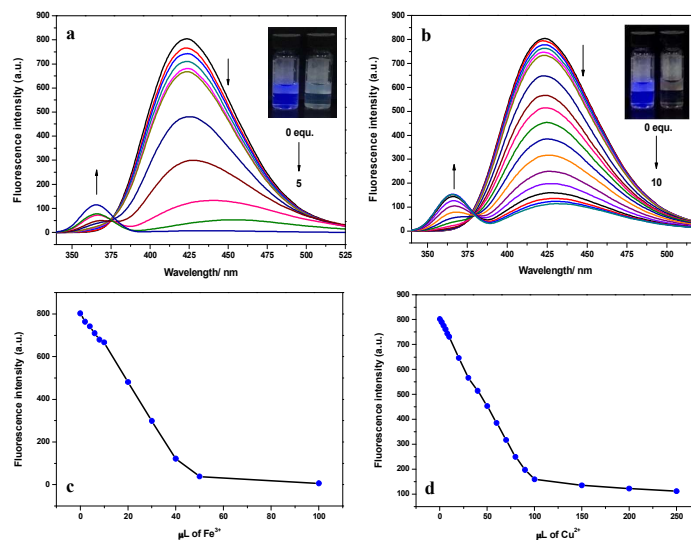


Fig. 5 Fluorescence spectrum of *m*-TAPA upon titration with aqueous solution of Fe^{3+} (a) and Cu^{2+} (b). A plot of changes of fluorescence intensity upon addition of Fe^{3+} (c) and Cu^{2+} (d) at 425 nm.

As shown in **Figure 6a, 6b**, free *m*-TAPA shows two absorption bands centered at 275 nm (band A) and 350 nm (band B), which can be assigned respectively as a π - π^* transition and an intramolecular charge transfer (ICT) band. Upon Fe^{3+} / Cu^{2+} addition (5 equiv.), band A increased gradually and obvious blue shift, while broad band B underwent a decrease and obvious red shift, which can be ascribed to the decrease of electron-donating ability induced by Fe^{3+} / Cu^{2+} coordination.^[49] In addition, a new band starts to appear (~ 400 nm) at the red side of the absorption spectrum of the free ligand and the absorbances increase with increasing gradually concentration of Fe^{3+} and Cu^{2+} ions, which indicated the different interaction pattern between partners of *m*-TAPA and Fe^{3+} / Cu^{2+} .^[50] A plot of absorbance depending on the concentration of Fe^{3+} and Cu^{2+} ions in the range from 0 to 5 equiv. as shown in **Fig. 6c and 6d**.

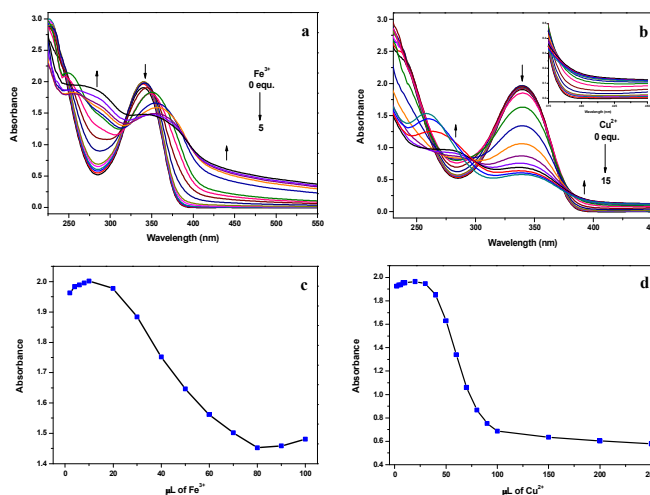


Fig. 6 UV-vis spectrum of *m*-TAPA (5×10^{-5} M, in CH_3CN) upon titration with aqueous solution of Fe^{3+} (a) and Cu^{2+} (b). Changes of UV absorbance upon addition of Fe^{3+} (c) and Cu^{2+} (d) at 337.5 nm.

To check further the practical applicability of *m*-TAPA as $\text{Fe}^{3+}/\text{Cu}^{2+}$ selective fluorescent sensor, the competitive experiments were performed in the presence of various metal ions. (Fig. 7 and 8). When *m*-TAPA was treated with 5 equiv. of Fe^{3+} and 10 equiv. of Cu^{2+} in the presence of the same concentration of other metal ions (Mg^{2+} , Zn^{2+} , K^+ , Ag^+ , Ni^{3+} , La^{3+} , Li^+ , Cd^+ , Sn^{2+} , In^{3+} , Fe^{2+} , Zr^{4+} and Al^{3+}), only Ag^+ ion inhibited about 55% of the interaction between *m*-TAPA and Fe^{3+} ion; K^+ ion inhibited about 70% of the interaction between *m*-TAPA and Cu^{2+} ion. This result is an added evidence for the high stability of the $\text{Fe}^{3+}/\text{Cu}^{2+}$ ion sensing, even in presence of other metal ions without any interference. Therefore, *m*-TAPA can be used as a selective fluorescent probe for Fe^{3+} and Cu^{2+} ions in practical environmental application.

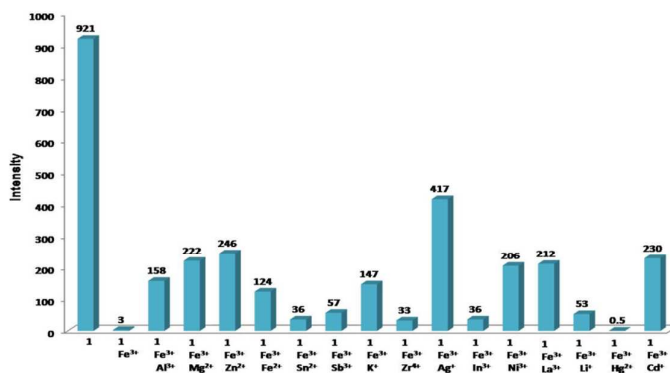


Fig. 7 Competitive selectivity of *m*-TAPA (1) toward Fe^{3+} in the presence of other metal ions (5 equiv.) with an emission of 425 nm.

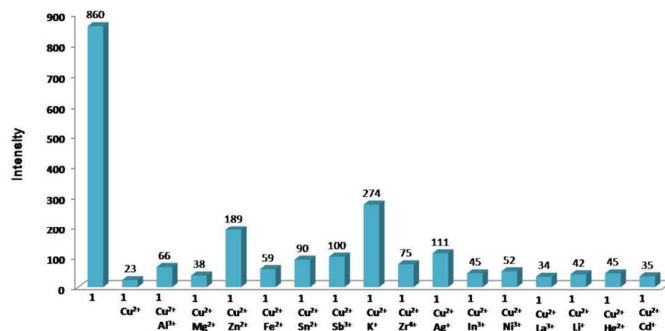


Fig. 8 Competitive selectivity of *m*-TAPA (1) toward Cu^{2+} in the presence of other metal ions (10 equiv.) with an emission of 425 nm.

Fig. 9 shows the Stern-Volmer analysis of the quenching experiment ($F_0 - F/F$ versus $[\text{Fe}^{3+}/\text{Cu}^{2+}]$). It is interesting to note the linear nature of the Stern-Volmer Plot over the Fe^{3+} and Cu^{2+} ions concentration range of 0-20 μM . The K_{SV} are $4.08 \times 10^4 \text{ M}^{-1}$ and $1.76 \times 10^4 \text{ M}^{-1}$ for $\text{Fe}^{3+}/\text{Cu}^{2+}$ ion, respectively. This phenomenon means the charge-transfer nature between *m*-TAPA and $\text{Fe}^{3+}/\text{Cu}^{2+}$ ion may be a static mechanism.^[51] Based on the results, The detection limit was then calculated with the equation: detection limit = $3\sigma_{bi}/m$, where σ_{bi} is the standard deviation of blank measurements and m is the slope of the intensity versus sample concentration. The detection limits of Fe^{3+} and Cu^{2+} ions with *m*-TAPA were 230 nM and 620 nM respectively, which is much lower than the maximum level (200 $\mu\text{g/L}$ to 1000 $\mu\text{g/L}$) of Fe^{3+} and ($\sim 20 \mu\text{M}$) of Cu^{2+} in drinking water permitted.

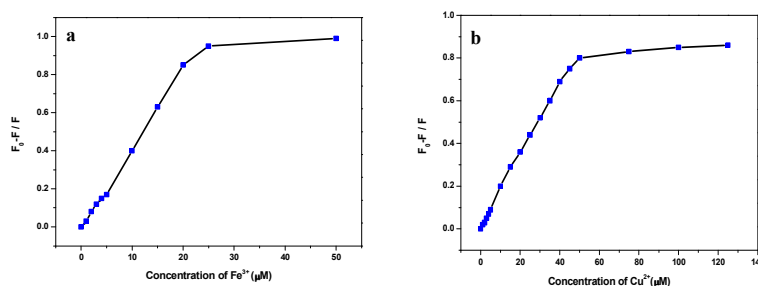


Fig. 9 Stern-Volmer plots for sensor *m*-TAPA using Fe^{3+} (a) and Cu^{2+} (b) as quencher at lower concentration.

pH effects on the fluorescence of probe (*m*-TAPA- Fe^{3+} and *m*-TAPA- Cu^{2+}) was investigated in CH_3CN . pH of the solution adjusted by adding of universal buffer. As shown in **Fig. 10**, *m*-TAPA show weak fluorescence in the pH range of 1.0-3.0, because of NH_2 groups of *m*-TAPA already had protonated. In pH range 4.0-8.0, the probe exhibited very good fluorescence behavior due to the protonation weakened about NH_2 groups of *m*-TAPA, but the emission intensity decreases at $\text{pH} > 8.0$ that indicates the *m*-TAPA- Fe^{3+} and *m*-TAPA- Cu^{2+} complexes were stable formed at high pH values. This result indicates that the sensor *m*-TAPA could be used for determination of Fe^{3+} and Cu^{2+} ions under common environmental condition.

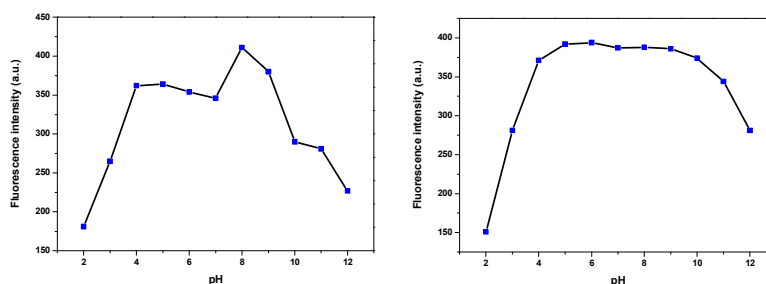


Fig. 10 Effect of pH on the Fe^{3+} and Cu^{2+} ion sensing ability by the *m*-TAPA at 425 nm.

The formation of aggregates of *m*-TAPA is supported by scanning electron microscopy (SEM) images in CH_3CN , which show the presence of very uniform spherical particles about 200nm (**Fig. 11a**). However, in the presence of Fe^{3+} and Cu^{2+} ion, the morphologies are changed into ununiformed size (**Fig. 11b, 11c**). These results demonstrate the interactions of *m*-TAPA with Fe^{3+} and Cu^{2+} ions possibly formed strong complexation led the break down of *m*-TAPA assembly morphology.

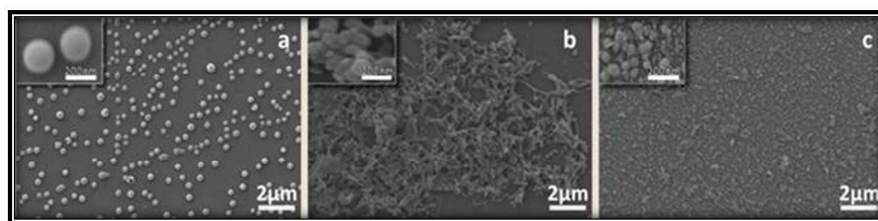


Fig. 11 Scanning electron microscopy (SEM) images of aggregates of compounds *m*-TAPA (a) in CH_3CN ; SEM images of [*m*-TAPA- Fe^{3+}] (b) and [*m*-TAPA- Cu^{2+}] (c).

Fig. 12 shows the interaction of *m*-TAPA with Fe^{3+} and Cu^{2+} ions investigated by ^1H NMR

spectroscopic titrations carried out in $\text{CD}_3\text{CN}/\text{D}_2\text{O}$. In the ^1H NMR titration experiments, with the molar ratio of self-assembled *m*-TAPA (10mg) and $\text{Fe}^{3+} / \text{Cu}^{2+}$ ion from 1:5 / 1:10, the NMR spectra exhibit fast exchange between the $\text{Fe}^{3+} / \text{Cu}^{2+}$ and *m*-TAPA. We found significant downfield shifts are observed for the peaks corresponding to the signal of protons of NH_2 groups, which can be recognized the presence of a strong charge transfer interaction between the electron-deficient $\text{Fe}^{3+} / \text{Cu}^{2+}$ and the electron-rich *m*-TAPA, leading to the formation of complex between $\text{Fe}^{3+} / \text{Cu}^{2+}$ and *m*-TAPA. Thus we inferred the possible binding mode as described in **Scheme 2**.

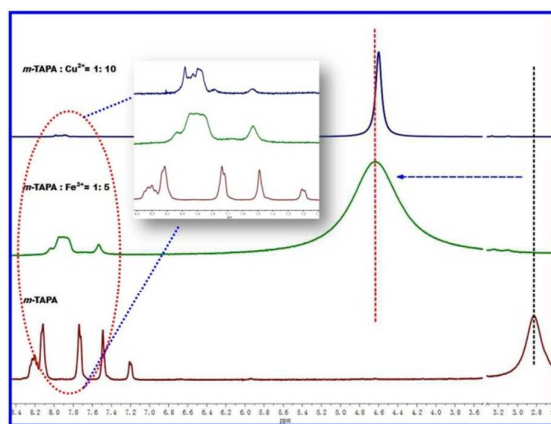
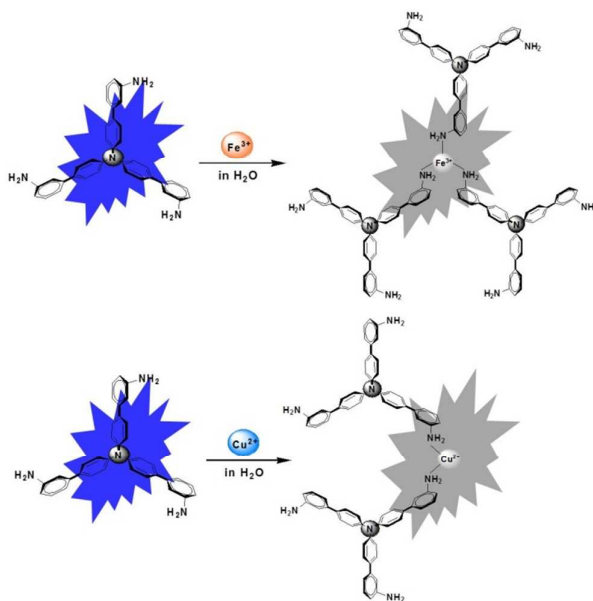


Fig. 12 ^1H NMR spectra of *m*-TAPA and $\text{Fe}^{3+} / \text{Cu}^{2+}$ in $\text{CD}_3\text{CN}/\text{D}_2\text{O} = 1:1$.



Scheme 2. Possible binding mode of probe (*m*-TAPA) with Fe^{3+} and Cu^{2+} ions.

To investigate the convenient application of sensor *m*-TAPA, test strips were prepared by immersing Thin Layer Chromatography (TLC) into a CH_3CN solution of *m*-TAPA (0.1 M). The test strips containing *m*-TAPA was utilized to sense Fe^{3+} and Cu^{2+} ion. As shown in **Fig. 13**, when $\text{Fe}^{3+} / \text{Cu}^{2+}$ was added on the test strips respectively, the obvious color change was observed under visible light (**Fig. 13b** and **c**). The fluorescence quenching were observed when the test strips are dipped into aqueous solutions of $\text{Fe}^{3+} / \text{Cu}^{2+}$ ion under the 365 nm UV lamp illumination (**Fig. 13e** and **f**). So, the test strips could conveniently detect Fe^{3+} and Cu^{2+} ions in aqueous solutions.

We also check the effect of various concentrations of Fe^{3+} / Cu^{2+} solution on the fluorescent TCL strip of *m*-TAPA (Fig. 14) by applying small spots of different concentrations of Fe^{3+} and Cu^{2+} (10 μL) on test strips. The visual fluorescence response of Fe^{3+} (a) and Cu^{2+} (b) at different concentrations by contact mode detection on test strips of *m*-TAPA as shown in Fig. 14. Dark spots of different strengths can be observed, which show the regulation of the quenching behavior of Fe^{3+} and Cu^{2+} (Fig. 14 ii-viii), which is also practically applicable by varying the concentration of the two metal ions even up to 5×10^{-13} M (Fig. 11 viii). However, no visible change is observed by applying blank solvent (CH_3CN) over the fluorescent test trips (Fig. 11 i).

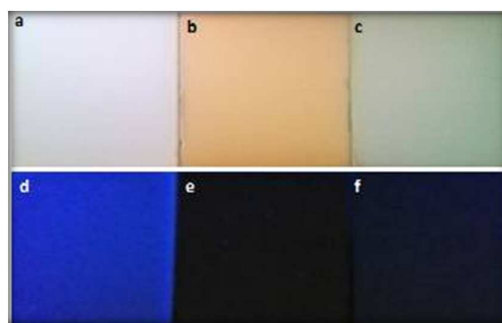


Fig. 13 Photographs of *m*-TAPA-coated test strips under visible light (a-c) and 365 nm UV (d-f) illumination. (a) and (d) Blank. (b) and (e) After dipping into solutions of Fe^{3+} in CH_3CN . (c) and (f) After dipping into solutions of Cu^{2+} in CH_3CN .

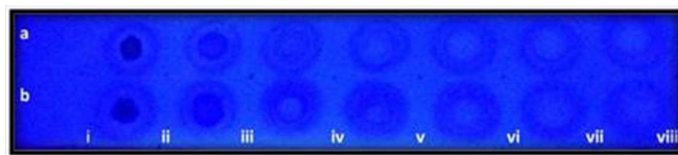


Fig. 14 Photograph of the fluorescence quenching of TAPA-coated test strips by Fe^{3+} (a) and Cu^{2+} (b) on contact mode (10 μL of Fe^{3+} and Cu^{2+} with a spot area of $\sim 0.2 \text{ cm}^2$) when viewed under 365 nm UV illumination. (i) blank, (ii) 5×10^{-3} M, (iii) 5×10^{-5} M, (iv) 5×10^{-7} M, (v) 5×10^{-9} M, (vi) 5×10^{-11} M, (vii) 15×10^{-12} M, (viii) 5×10^{-13} M.

4. Conclusions

In summary, we have prepared a simple but effective fluorescent sensor, *m*-TAPA, for Fe^{3+} / Cu^{2+} . The sensor is highly selective and hardly interfered by other metal ions with the detection limit of Fe^{3+} and Cu^{2+} ions were 230 nM and 620 nM respectively. The K_{SV} value of Fe^{3+} and Cu^{2+} were calculated as $4.08 \times 10^4 \text{ M}^{-1}$ and $1.76 \times 10^4 \text{ M}^{-1}$ respectively. These results indicate that *m*-TAPA could meet the selective requirements for environmental application and can be sensitive enough to detect Fe^{3+} / Cu^{2+} ion in environmental water samples, even in drinking water. Additionally, *m*-TAPA-coated TCL strips serve as a convenient, low-cost method for detection of Fe^{3+} / Cu^{2+} ion at nanomolar range.

Acknowledgements

This work was supported the National Natural Science Foundation of China (no. 21202133, 21174114, 21361023). We also thank Key Laboratory of Eco-Environment-Related Polymer Materials (Northwest Normal University), the Ministry of Education Scholars Innovation Team (IRT 1177) for financial support.

References

- [1] B. Valeur, I. Leray, *Coord. Chem. Rev.* 2000, **205**, 3-40.
- [2] Q. Zhao, F. Li, C. Huang, *Chem. Soc. Rev.* 2010, **39**, 3007-3030.
- [3] M. Angelova, S. Asenova, V. Nedkova, R. K. Kolarova, *Trakia. J. Sci.* 2011, **9**, 88-98.
- [4] R. Ajlec, J. Stupar, *Analyst* 1989, **114**, 137-142.
- [5] P. B. Pati, S. S. Zade, *Inorg. Chem. Commun.* 2014, **39**, 114-118.
- [6] L. S. Huang, K. C. Lin, *Spectrochim. Acta B* 2001, **56**, 123-128.
- [7] R. De Marco, J. Martizano, *Talanta* 2008, **75**, 1234-1239.
- [8] A. Bobrowski, K. Nowak, J. Zarebski, *Anal. Bioanal. Chem.* 2005, **382**, 1691-1697.
- [9] L. Qiu, C. C. Zhu, H. C. Chen, M. Hu, W. J. He, Z. J. Guo, *Chem. Commun.* 2014, **50**, 4631-4634.
- [10] S. L. Belli, A. Zirino, *Anal. Chem.* 1993, **65**, 2583-2589.
- [11] H. Tapiero, D. M. Townsend, K. D. Tew, *Biomed. Pharmacother.* 2003, **57**, 386-398.
- [12] R. Uauy, M. Olivares, M. Gonzalez, *Biomed. Pharmacother.* 2003, **57**, 134-144.
- [13] J. Huller, M. T. Pham, S. Howitz, *Sensor. Actuat. B* 2003, **91**, 17-20.
- [14] D. J. Waggoner, T. B. Bartnikas, J. D. Gitlin, *Neurobiol. Dis.* 1999, **6**, 221-230.
- [15] K. J. Barnham, C. L. Masters, A. I. Bush, *Nat. Rev. Drug Discov.* 2004, **3**, 205-214.
- [16] D. R. Brown, H. Kozlowski, *Dalton Trans.* 2004, **13**, 1907-1917.
- [17] P. G. Georgopoulos, A. Roy, M. J. Yonone-Lioy, R. E. Opiekun, P. J. Lioy, *J. Toxicol. Environ. Health Part B* 2001, **4**, 341-394.
- [18] McMichael et al. Guidelines for Drinking Water Quality, World Health Organization: Geneva, **1996**.
- [19] E. Oken, R. O. Wright, K. P. Kleinman, D. Bellinger, C. J. Amarasiriwardena, H. Hu, J. W. Rich-Edwards, M. W. Gillman, 2005, **113**, 1376-1380.
- [20] W. C. Prozialeck, J. R. Edwards, J. M. Woods, *Life Sci.* 2006, **79**, 1493-1506.
- [21] O. Kaplan, N. C. Yildirim, N. Yildirim, N. Tayhan, *Turkey, E-J. Chem.* 2011, **8**, 276-280.
- [22] T. V. Tam, N. B. Trung, H. R. Kim, J. S. Chung, W. M. Choi, *Sens. Actuators, B* 2014, **202**, 568-573.
- [23] D. Udhayakumari, S. Velmathia, Y. M. Sung, S. P. Wu, *Sens. Actuators, B* 2014, **198**, 285-293.
- [24] M. Royzen, Z. Dai, J. W. Canary, *J. Am. Chem. Soc.* 2005, **127**, 1612-1613.
- [25] N. Shao, J. Jin, H. Wang, Y. Zhang, R. Yang, W. Chan, *Anal. Chem.* 2008, **80**, 3466-3475.
- [26] N. Li, Y. Xiang, A. Tong, *Chem. Commun.* 2010, **46**, 3363-3365.
- [27] Z. Q. Guo, W. Q. Chen, X. M. Duan, *Org. Lett.* 2010, **12**, 2202-2205.
- [28] X. Chen, T. Pradhan, F. Wang, J. S. Kim, J. Yoon, *Chem. Rev.* 2012, **112**, 1910-1956.
- [29] J. L. Bricks, A. Kovalchuk, C. Trieflinger, M. Nofz, M. Büschel, A. I. Tolmachev, J. Daub, K. Rurack, *J. Am. Chem. Soc.* 2005, **127**, 13522-13529.
- [30] B. Wang, J. Hai, Z. Liu, Q. Wang, Z. Yang, S. Sun, *Angew. Chem. Int. Ed.* 2010, **49**, 4576-4579.
- [31] D. Wei, Y. Sun, J. Yin, G. Wei, Y. Du, *Sens. Actuators, B* 2011, **160**, 1316-1321.
- [32] Z. Yang, M. She, B. Yin, J. Cui, Y. Zhang, W. Sun, J. Li, Z. Shi, *J. Org. Chem.* 2012, **77**, 1143-1147.
- [33] V. Bhalla, N. Sharma, N. Kumar, M. Kumar, *Sens. Actuators, B* 2013, **178**, 228-232.
- [34] M. Zhang, Y. Gao, M. Li, M. Yu, F. Li, L. Li, M. Zhu, J. Zhang, T. Yi, C. Huang,

Tetrahedron Letters 2007, **48**, 3709-3712.

- [35] J. Y. jung, S. L. Han, J. Chun, C. Lee, J. Yoon, *Dyes Pigments* 2012, **94**, 423-426.
- [36] X. X. He, J. Zhang, X. G. Liu, L. Dong, D. Li, H. Y. Qiu, S. C. Yin, *Sens. Actuators, B* 2014, **192**, 29-35.
- [37] S. Wang, G. Men, L. Zhao, Q. Hou, S. Jiang, *Sens. Actuators, B* 2010, **145**, 826-831.
- [38] K. M. K. Swamy, M. J. Kim, H. R. Jeon, J. Y. Jung, J. Yoon, *Bull. Korean Chem. Soc.* 2010, **31**, 3611-3616.
- [39] N. Singh, N. Kaur, C. N. Choitir, J. F. Callan, *Tetrahedron Lett.* 2009, **50**, 4201-4204.
- [40] L. Wang, H. Li, D. Cao, *Sens. Actuators, B* 2013, **181**, 749-755.
- [41] M. W. wang, J. W. wang, W. Xue, A. Wu, *Dyes Pigments* 2013, **97**, 475-480.
- [42] Y. W. Choi, G. J. Park, Y. J. Na, H. Y. Jo, S. A. Lee, G. R. You, C. Kim, *Sens. Actuators, B* 2014, **194**, 343- 352.
- [43] K. D. Bhatt, H. S. Gupte, B. A. Makwana, D. J. Vyas, D. Maity, V. K. Jain, *J. Fluoresc.* 2012, **22**, 1493-500.
- [44] B. K. Kanungo, M. Baral, R. K. Bera, S. K. Sahoo, *Monatsh Chem.* 2010, **141**, 157-168.
- [45] N. Miyaura, A. Suzuki, *Chem. Rev.* 1995, **95**, 2457-2483.
- [46] L. J. Fan, Y. Zhang, C. B. Murphy, S. E. Angell, M. F. L. Parker, B. R. Flynn, *Coord. Chem. Rev.* 2009, **253**, 410-422.
- [47] N. Demas, G. A. Grosby, *J. Phys. Chem.* 1971, **75**, 991-1024.
- [48] A. S. F. Chipem, S. K. Behera, G. Krishnamoorthy, *Sens. Actuators, B* 2014, **191**, 727-733.
- [49] Z. P. Liu, C. L. Zhang, X. Q. Wang, W. J. He, Z. J. Guo, *Org. Lett.* 2012, **4**, 4378-4381.
- [50] S. Pramanik, V. Bhalla, M. Kumar, *ACS Appl. Mater. Interfaces* 2014, **6**, 5930-5939.
- [51] E. Ballesteros, D. Moreno, T. Gomez, T. Rodriguez, J. Rojo, M. G. Valverde , T. Torroba, *Org. Lett.* 2009, **11**, 1269-1272.